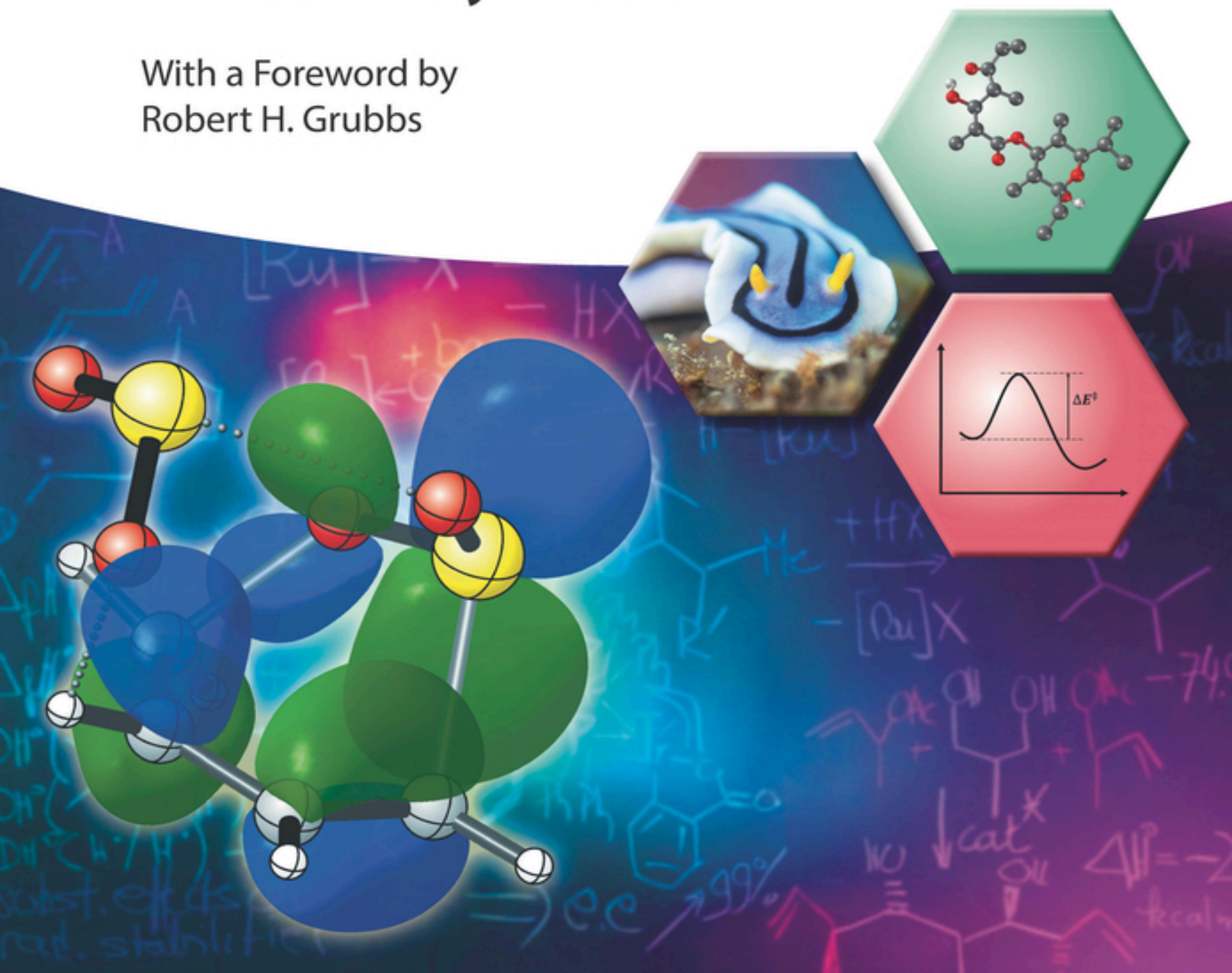Pierre Vogel and Kendall N. Houk

Organic Chemistry

Theory, Reactivity and Mechanisms in Modern Synthesis

With a Foreword by
Robert H. Grubbs

Organic Chemistry

Organic Chemistry

Theory, Reactivity and Mechanisms in Modern Synthesis

With a Foreword by Robert H. Grubbs

Pierre Vogel

Kendall N. Houk

WILEY-VCH

Authors

Prof. Pierre Vogel
EPFL
SB-DO
Avenue F.-A. Forel 2
1015 Lausanne
Switzerland

Prof. Kendall N. Houk
Dept. of Chemistry and Biochemistry
University of California
Los Angeles, CA 90095–1569
United States

Cover: The cover features a computed transition state structure with frontier molecular orbitals for the Diels-Alder reaction of SO2 and butadiene, catalyzed by another SO2 (J. Am. Chem. Soc. 1998, 120, 13276–13277). Pierre Vogel established the mechanism of this reaction and applied it to the total synthesis of natural product (-)-dolabriferol (Angew. Chem. Int. Ed. 2010, 49, 8525–8527), the structure of which shown in the green hexagon, originally from dolabrifera dolabrifera the sea slug (also shown in its vivid UCLA colors). A potential energy diagram in the red hexagon and blackboard writings in the background (courtesy P. Vogel) are key concepts discussed extensively in this book to describe mechanism and reactivity.

Contents

Preface

Scientists interested in molecular sciences with basic knowledge in chemistry might retain this book as their second textbook in organic chemistry. This book is also a reference manual for chemists and chemical engineers who invent new reactions and design new procedures for the conversion of simple chemicals into high value-added materials. All answers to the problems in this book, and references to the original literature relevant to the problems, are contained in our companion Workbook of the same name as this book. We plan to produce another book describing reaction intermediate and their reactions, as well as solvation and weak molecular interactions.

Chemistry is an empirical science but is increasingly influenced by understanding and prediction. Before starting a new experiment in the laboratory, a chemist would like to know the following:

(1) Is the reaction possible thermodynamically?
(2) How long is it going to take?
(3) What will be the properties of the reaction products?

This book introduces and documents models that enable chemists to answer these questions and to understand the reasons behind the answers. The methods will be illustrated with a large number of reactions that have a wide practical value in synthesis and biology. Reactions involving organic, organometallic, and biochemically important reactants and catalysts will be presented. We teach the tools that can be used to understand Nature and to control and create new chemistry to achieve a better world. Given specific combinations of solvent, concentration, temperature, pressure, the presence or absence of catalysts and inhibitors, light, or other types of radiation, a given system of reactants will be converted into a mixture of products. Rates of product formation or attainment of equilibria define chemical reactivity. Living systems are made of ensembles of molecules that are connected through ensembles of chemical reactions. We like to think of most chemists, biochemists, molecular biologists,

material physicists, and all those who study molecular phenomena as molecular scientists. They (and we) try to understand Nature and to imitate its efficiency and diversity. Molecular scientists, especially chemists, are not passive observers. Chemists can even surpass Nature, by inventing new molecular entities – chemicals! – and new reactions that have not been observed yet in our Universe, at least on our planet! Through chemical knowledge, combined with serendipity, molecular scientists are creating a new world, consisting of useful chemicals such as pharmaceuticals, crop protection agents, food protective agents, perfumes, aromas, optical and electronic materials, fabric for clothes and other applications, construction materials for energy-saving houses and vehicles, and coatings and paints. The new world of nanoscience is molecular and supramolecular science. Chemists – many of whom are really molecular engineers – strive to obtain targeted compounds by chemical or biochemical synthesis as rapidly as possible and by the most economic routes possible. Nowadays, chemists invent procedures that are environmental friendly and contribute significantly to a more sustainable development, with more respect for the limited resources of our Earth.

Chemical structures, stability, and reactivity are governed by thermodynamics (Chapters 1 and 2) and kinetics (Chapter 3). Thermodynamics dictates how atoms assemble into stable molecules and how molecules assemble into supramolecular systems. Kinetics quantitates the rates at which molecules are transformed into other molecules or assemblies of molecules under specific conditions. Our preface gives a brief history of chemistry and shows how heat exchange is fundamental to produce and modify chemicals. All chemical changes are accompanied by absorption (endothermic reactions: $\Delta_r H^T > 0$) or release (exothermic reactions: $\Delta_r H^T < 0$) of heat. The heat of any reaction can be measured by calorimetry. It is the variation of enthalpy ($H = E + PV$) during the time between when the reactants are mixed and when the equilibrium with the products is reached, for a

reaction at constant temperature and pressure. The first reaction used by man was fire, the combustion of dry grass or wood in the air to produce carbon dioxide + water (fumes), heat, and light next to ashes that are inorganic carbonates, hydroxides, and oxides. Any chemical or biochemical reaction equilibrates reactants (also called substrates and reagents, or starting materials) with products (and coproducts). At temperature T, the reaction equilibrium is characterized by an equilibrium constant, K^T, which depends on the nature of reactants and products and on the reaction conditions (temperature, pressure, concentration, and solvent). For instance, if equilibrium $\mathbf{A} + \mathbf{B} \rightleftarrows \mathbf{P} + \mathbf{Q}$ (one molecule of reactant $\mathbf{A}$ and one molecule of reactant $\mathbf{B}$ equilibrate with one molecule of product $\mathbf{P}$ and one molecule of coproduct $\mathbf{Q}$) can be considered as an ideal solution, $K^T = [\mathbf{P}][\mathbf{Q}]/[\mathbf{A}]][\mathbf{B}]$; $[\mathbf{P}]$, $[\mathbf{Q}]$, $[\mathbf{A}]$, and $[\mathbf{B}]$ are the concentration of products $\mathbf{P}$, coproduct $\mathbf{Q}$, and of reactants $\mathbf{A}$ and $\mathbf{B}$, respectively. Under constant pressure and temperature, the Gibbs free energy of the reaction $\Delta_r G^T = -RT \ln K^T = \Delta_r H^T - T\Delta_r S^T$, with $\Delta_r H^T$ = heat of the reaction and $\Delta_r S^T$ = entropy variation of the reaction (or reaction entropy). Those reactions that convert reactants into products with a good conversion have $K^T > 1$ and correspond to $\Delta_r G^T < 0$. They are said to be exergonic. For endergonic reactions with $K^T < 1$, $\Delta_r G^T > 0$, products can be obtained with good conversion if they can be separated selectively from the reactants (e.g. precipitation of one product from an homogenous solution and evaporation of one product or coproduct from the solid or liquid reaction mixture) they are equilibrating with (equilibrium shift). As a general rule, condensations that convert small molecules into larger molecules (the number of molecules diminishes from reactants to products) have negative reaction entropies ($\Delta_r S^T < 0$) and fragmentations that convert large molecules into smaller molecules (the number of molecules increases from reactants to products) have positive entropies ($\Delta_r S^T > 0$). The heat absorbed or released in a reaction, $\Delta_r H^T$, represents a powerful tool to understand chemical transformations at the molecular level (molecular chemistry). This textbook shows how thermochemical data such as standard (1 atm, 25 °C) heats of formation ($\Delta_f H°$), standard entropies ($S°$), homolytic bond dissociation enthalpies ($DH°(\mathrm{R^{\cdot}/X^{\cdot}})$), gas-phase heterolytic bond dissociation enthalpies ($DH°(\mathrm{R^+/X^-})$), gas-phase acidities ($\Delta_f G°(\mathrm{A-H} \rightleftarrows \mathrm{A^-} + \mathrm{H^+})$ and proton affinities (PA $= DH°(\mathrm{A^-/H^+})$), ionization energies (EIs), electron affinities (−EAs), and solution acidity constants (K_a, pK_a) from the literature (tables of data collected before references to Chapter 1, p. 53–91) and online data banks can be used to understand molecular properties and reaction equilibria, including equilibria involving charged species (Chapters 1 and 2). We give simple techniques ("back of the envelope methods") that allow one to estimate thermochemical data of reactants, products, and reactive intermediates for which these data have not been measured. This permits one to evaluate the equilibrium constants of any organic reactions for systems that can be considered as ideal gases or ideal solutions, which is the case for a large number of organic and organometallic reactions run in the laboratory. Equilibria between two phases find multiple applications in preparative chemistry (e.g. solution/solid: crystallization) and analytical chemistry (e.g. solid of liquid stationary phase/mobile liquid or gaseous phase: chromatography). They are exploited in the resolution of racemates into enantiomers and in thermodynamically controlled deracemizations. Isotopic substitution affects equilibria and gives important information about bonding in molecules.

A chemical or biochemical reaction is characterized by its rate of reaction and its rate of law (Chapter 3). Both depend on the nature of the reactants, the reaction mechanism, and the reaction conditions (temperature, pressure, concentration, solvent, and presence of catalyst(s) and inhibitor(s)). For instance, for the irreversible reaction (with a large K^T value) $\mathbf{A} + \mathbf{B} \rightarrow \mathbf{P} + \mathbf{Q}$, the disappearance of reactant $\mathbf{A}$ may follow the second-order rate law $d[\mathbf{A}]/dt = -k[\mathbf{A}][\mathbf{B}]$ with k being the rate constant. Chemical kinetics (the measure of reaction rate constant k as a function of temperature) allows one to evaluate activation parameters using the empirical Arrhenius relationship: $k = A\,e^{-E_a/RT}$. This gives the empirical activation parameters E_a = activation energy and A = frequency factor. Eyring considers the transition state of a reaction to be an activated complex in a quasi-equilibrium with the reactants (equilibrium $\mathbf{A} + \mathbf{B} \rightleftarrows [\mathbf{A} \cdot \mathbf{B}]^{\ddagger}$). Thermodynamics applied to this equilibrium defines the Eyring activation parameters $\Delta^{\ddagger}H$ = activation enthalpy ($\Delta^{\ddagger}H = E_a - RT$), $\Delta^{\ddagger}S$ = activation entropy, $\Delta^{\ddagger}G = \Delta^{\ddagger}H - T\Delta^{\ddagger}S$ = free energy of activation and permits the delineation of mechanistic limits (nature of the transition state of the rate-determining step) at the molecular level. Conversely, if the reaction mechanism is known, the activation parameters can be estimated and can be used to predict under which conditions (pressure, concentration, and temperature) the reaction will occur and how long it will take for a given conversion. For systems in solution, rates can be enhanced or reduced by applying high pressures. This provides activation volumes ($\Delta^{\ddagger}V$) that are important information about reaction mechanisms. Rates of reaction also depend on chirality,

a phenomenon exploited in asymmetric synthesis (the preparation of enantiomerically enriched or pure compounds) that is extremely important in modern medicinal chemistry and material sciences. The most important tools of modern asymmetric synthesis will be presented (Section 3.6) and illustrated throughout the book. The question of how chirality appeared on Earth will be addressed (e.g. asymmetric autocatalysis). Isotopic substitution can also affect the rate of a given reaction. Kinetic isotopic effects are powerful tools to study reaction mechanisms.

Quantum mechanical calculations have become routine molecular models for chemists, biochemists, and biologists. They are the basis of simpler molecular orbital theories (Hückel method, Coulson and Longuet–Higgins approach, and the perturbation of molecular orbital (PMO) theory) that help to describe molecular properties and their reactions and to establish bridges between molecular organic, organometallic, and inorganic chemistry (Chapter 4 and Section 7.6). Notions such as conjugation, hyperconjugation, Hückel and Heilbronner aromaticity, and antiaromaticity find a solid basis in quantum mechanical calculations. Modern computational methods have proven to be a robust way to establish mechanisms; continuing increases in computer power and the accuracy of methods make computations an increasingly valuable way to establish the favored mechanisms of reactions.

Mechanistically, reactions can be classified into one-step and multistep reactions. Pericyclic reactions (electrocyclic ring closures and openings, cycloadditions and cycloreversions, cheletropic additions and eliminations, sigmatropic rearrangements, dyotropic rearrangements, and ene-reactions) for long were considered as "no-mechanism reactions." They have played a key role in our understanding of reaction mechanisms (concerted vs. nonconcerted mechanism, importance of diradical and zwitterion intermediates, and the diradicaloid theory for transition states) and chemical reactivity in general (Chapter 5). These reactions are extremely useful synthetic tools, including in asymmetric synthesis.

Without sunlight, green plants do not grow. The color of natural or painted objects fades away when they are exposed to the sun. Light can induce chemical and biochemical reactions. The concepts that enable us to understand the interaction of light with organic compounds and how light can make them to react in ways different from under heating are presented in Chapter 6. Interpretation of the UV–visible spectra of organic molecules has played a major role in structural analytical chemistry and in the design of dying agents.

Phenomena such as fluorescence and phosphorescence, chemiluminescence, and bioluminescence teach us about the nature of the electronically excited state of molecules (singlet vs. triplet states) and their unimolecular and bimolecular reactions. The photochemistry of functional compounds (isomerization, bond cleavage, cycloadditions, photooxidations, photocatalysis, etc.) represents a powerful tool of preparative chemistry. The photoreactions in which light initiates chain processes, or induces electronic transfers, are extremely useful. Photoinduced electron transfer is fundamental to dye-sensitized solar cells.

Humans have survived eating animals, plants, and parts of plants. Animals also survive consuming other animals or plants. Photosynthesis ($n\text{CO}_2 + n\text{H}_2\text{O} \rightarrow \text{C}_n\text{H}_{2n}\text{O}_2$ [carbohydrates]) in plants has for long produced more biomass than necessary for all living species on Earth. Geological phenomena have permitted the storage of large parts of past biomass underground in the form of coal, tars, petroleum, and natural gas (fossil fuels). When human beings started to control fire (c. 1.6×10^6 years ago), they found that heat can be used to convert biomass and minerals into valuable materials. This is obvious with the development of pottery and metallurgy, which represent the first chemical industries. Then, biomass fermentative processes (wine and beer) and wood distillation have become the next chemical industries. The Industrial Revolution, which began in late 1700s in the UK, has led to mass production and, consequently, to a new consumer society. The processes applied have produced a lot of unwanted secondary products (waste) and are consuming larger and larger amounts of energy, mostly burning fossil fuels. This cannot be continued without affecting irreversibly our environment (emission of CO_2, nitrogen oxides, methane, nanoparticles, etc.) and our quality of life. It is urgent to develop cleaner processes that do not reject any waste and require much less energy. Today, chemists invent new procedures that contribute to a more sustainable economy ("green chemistry"). The new procedures rely upon new reactions that are atomic economically (no coproducts, no secondary products, and no solvent) and require no heating or no cooling. Most chemists create new compounds by combining reagents in C-heteroatom or C—C bond forming reactions. For 150 years, this required polar starting materials (organometallic reagents and halogenated compounds) that can combine in substitution and addition reactions. Quite often, these reactions produce coproducts and side products that cannot be recycled in an economical manner. Organometallic reagents and

halogenated starting materials require several synthetic steps for their obtainment from available resources. For instance, the very much applied Friedel–Crafts acylation Ar–H (aromatic hydrocarbon) + $RCOCl + AlCl_3 \rightarrow ArCOR + HAlCl_4$ first requires the conversion $RCOOH + SOCl_2 \rightarrow RCOCl + SO_2 + HCl$. The process produces HCl and SO_2 washed with alkaline water-producing large amounts of waste. Another example is the classical preparation of secondary alcohols from alcohols and aldehydes using Grignard reagents, e.g. $R–Br + Mg \rightarrow RMgBr$; then $R'CHO + RMgBr \rightarrow RCH(OMgBr)R'$, then $RCH(OMgBr)R' + H_2O \rightarrow RCH(OH)R' + Mg(OH)Br$ (waste). In general, bromides are not readily available; they can be made according to $ROH + BBr_3 \rightarrow R–Br + B(OH)Br_2$ (waste). Mg and other reactive metals such as Li, Na, and K require a lot of energy for their preparation. Direct hydrocarbation of unsaturated compounds is much more atomic economically. Examples are the aldol reaction ($RCHO + R'CH_2COR'' \rightleftarrows RCH(OH)–CH(R')–COR''$) and many newer reactions presented in this book such as $RCH_2OH + CH_2 = CHR' \rightarrow RCH(OH)–CH(Me)R'$. The latter reaction can generate four possible stereoisomers (two diastereomers as racemic mixtures) as two new stereogenic centers are created. If the reaction should not be regioselective, one further isomeric product can form. In this latter case, $RCH_2OH + CH_2 = CHR' \rightarrow RCH(OH)–CH_2CH_2R'$ (racemate). We shall see that suitable catalysts are available that make it possible to form only one major product enantiomerically enriched, if not enantiomerically pure. Emphasis today is to use readily available starting materials extracted from renewable resources such as the biomass and chemicals derived from it. For that, chemists invent new catalysts that are either heterogeneous (do not dissolve in the reactants and solvent) of homogeneous (dissolve in the reactants and solvent) and perform better and better. Chapters 7 and 8 are devoted to catalytic reactions with examples applied in the bulk chemical industry and many others applied in fine chemistry, including in the asymmetric synthesis of compounds of biological interest. These chapters give the concepts to understand how homogeneous catalysts work at the molecular level. They should help the reader to invent further catalysts and new reactions that are high yielded, chemoselective (e.g. hetero-Diels–Alder reaction vs. (4+1)-cheletropic addition of SO_2 to 1,3-dienes) site-selective (selective between similar functions of multifunctional reactants), regioselective (e.g. Markovnikov or anti-Markovnikov orientation), diastereoselective (e.g. *erythro* or *threo* through *anti* or *syn* addition), and enantioselective (e.g. π-face

selective), requiring no heating or cooling and that are completely atomic economical.

History, enthalpy, and entropy in the transformation of matter

As mentioned above, fire is the oldest reaction used by man (most of the material presented in this section can be found in the Internet: Wikipedia, the free encyclopedia, www.wikipedia.org). The earliest reactions induced by heat has been the smelting of lead and tin (6500 BC). A common lead ore is galena (PbS). When heated in the air, lead sulfite is obtained (equilibrium: $2PbS + 3O_2 \rightleftarrows 2PbSO_3$). Oxygen of air burns lead sulfide in a exothermic reaction that condenses five molecules into two, a process disfavored entropically, but it occurs because of the exothermicity ($\Delta_r H^T < 0$) of the reaction, which pays for the entropy cost ($-T\Delta_r S^T > 0$). Upon heating, lead sulfite decomposes into solid lead oxide and volatile sulfur dioxide (equilibrium $PbSO_3 \rightleftarrows PbO + SO_2$). Although $PbSO_3$ is a stable compound at room temperature, heating induces its fragmentation into two smaller molecules. At high temperature, the reaction is favored entropically and also by the "Le Châtelier principle" (SO_2 flies away from the reaction mixture). This reaction is like limestone calcining: $CaCO_3 \rightarrow CaO + CO_2$. Incomplete combustion of charcoal produces carbon monoxide, CO, which reduces lead oxide into metallic lead and CO_2 according to equilibrium $PbO + CO \rightleftarrows Pb + CO_2$. The variation of entropy for this reaction is small as it does not change the number of molecules between reactants and products. Metallic lead forms because the C—O bonds in CO_2 are stronger than the Pb—O bond in solid lead oxide. This is demonstrated by the heats of combustion $\Delta_r H^{298\,K}(CO + \frac{1}{2}O_2 \rightleftarrows CO_2$, gas phase) $= -67.6\,kcal\,mol^{-1}$ and $\Delta_r H^{298\,K}(Pb(solid) + \frac{1}{2}O_2 \rightleftarrows PbO(solid) = -52.4\,kcal\,mol^{-1}$. Overall, the reduction of lead oxide by CO is exothermic by $\Delta_r H^{298\,K}(PbO(solid) + CO(gas) \rightleftarrows Pb(solid) + CO_2$ (gas)) $= -15.2\,kcal\,mol^{-1}$ (NIST WebBook of Chemistry, National Institute of Standards and Technology, http://webbook.nist.gov/chemistry/). The Bronze age started with the discovery that a better metallic material, the alloy bronze, can be obtained by smelting tin (e.g. cassiterite: SnO_2) and copper (e.g. malachite: $[Cu_2CO_3(OH)_2]$, chalcocite: CuS, chalcopyrite: $CuFeS_2$) ores together with carboneous materials such as charcoal (c. 3500 BC). Iron Age (c. 1500 BC) started with the discovery of smelting of iron oxide with charcoal. Overall, $\Delta_r H^{298\,K}(2Fe_2O_3(solid) +$

$3C(\text{solid}) \rightleftarrows 4Fe(\text{solid}) + 3CO_2(\text{gas})) = 112.6\,\text{kcal mol}^{-1}$, which is highly endothermic, but profits of the positive entropy of reaction and of the le Châtelier principle (formation of CO_2 that flies away) at high temperature. Concomitant burning of charcoal compensates for the overall endothermicity. The process implies several reactions: First $4C + 2O_2 \rightarrow 4CO$, then three successive reductions with CO: $3Fe_2O_3 + CO \rightarrow 2Fe_3O_4 + CO_2$; $Fe_3O_4 + CO \rightarrow 3FeO + CO_2$; $FeO + CO \rightarrow Fe + CO_2$. The overall process $Fe_2O_3 + 4C + 2O_2 \rightleftarrows 2Fe + 3CO_2 + CO$ is exothermic by c. $-110\,\text{kcal mol}^{-1}$.

Fermentative processes (biochemical transformations catalyzed by a microorganism; e.g. $C_6H_{12}O_6$ (D-glucose in water) $\rightarrow 2CH_3CH_2OH$ (ethanol in water) $+ 2CO_2$, $\Delta_r H^{298\,K} = -17.8\,\text{kcal mol}^{-1}$) such as beer and wine making have been known for at least 8000 years. Acetic acid (CH_3COOH, IUPAC name: ethanoic acid) in the form of sour wine has also been known for the same time. The process of distillation permits the isolation of pure organic chemicals such as ethanol and acetic acid as described for the first time by the Alexandrians (500 BC). One of the earliest organic chemistry reaction (2800 BC) is the formation of soap (e.g. sodium stearate: $Me(CH_2)_{16}COONa$, sodium palmitate: $Me(CH_2)_{14}COONa$) obtained by reacting olive oil or palm oil with ashes (NaOH, Na_2CO_3). The reaction ($RCOOCH_2$–CH(OCOR)–CH_2OCOR (triglyceride) $+ 3NaOH \rightleftarrows 3RCOONa$ (soap) $+ HOCH_2$–CH(OH)–CH_2OH (glycerin) $+$ heat) occurs already at room temperature. Soap manufacturers have observed very early that heating the reaction mixture would accelerate the process. The rate of the reaction increases with temperature. It also depends on the type of ashes used for saponification. Some are more active (contain more NaOH) than others. Aged ashes are less reactive because they contain more hydrogenocarbonates and carbonates. This results from the slow absorption of CO_2 present in the air, which reacts with oxides, hydroxides (e.g. $NaOH + CO_2 \rightleftarrows NaHCO_3$). At low temperature, condensation is favored thermodynamically, whereas the reverse reaction, fragmentation (decarboxylation), is favored upon heating.

Charcoal required by the early metallurgy was produced by partial combustion of wood. With time, various techniques of wood pyrolysis (also called destructive distillation) have been developed, which have led to the production and isolation of several chemicals such as methanol, turpentine (volatiles), and tar (nonvolatiles). Turpentine (from pine tree), used as paint thinner, was prepared first by the Persians (3000 BC). It is mentioned in European literature in the thirteenth century. It is mostly composed of $(-)$-α-pinene (European pine), $(+)$-α-pinene (North American pine), β-pinene, $(+)$-3-carene, and lesser amounts of $(-)$-camphene, dipentene (racemic limonene $= (\pm)$-limonene $= 1:1$ mixture of $(+)$-limonene and $(-)$-limonene), and α-terpinolene (Figure 1). Except for α-terpinolene, these monoterpenes are chiral compounds that can be obtained with high enantiomeric purity. These odorous compounds are found in several plants (essential oils). Nowadays, they are used as starting materials in the perfume industry and in the asymmetric synthesis of drugs (part of the chiral pool).

IUPAC names: $(-)$-α-pinene $= (-)$-(1S,5S)-2,6,6-trimethylbicyclo[3.1.1]hept-2-ene; $(-)$-β-pinene: $(-)$-(1S,5S)-6,6-dimethyl-2-methylidenebicyclo[3.1.1] heptane; $(+)$-3-carene: $(+)$-(1S,6S)-3,7,7-trimethylbicyclo[4.1.0]hept-3-ene; $(-)$-camphene: $(-)$-(1S,4R)-2,2-dimethyl-3-methylidenebicyclo[2.2.1]heptane (as these rigid bicyclic hydrocarbons with two stereogenic centers cannot have diastereomers, they exist as two enantiomers only, the second stereomarker can be dropped); $(+)$-limonene (orange odor): $(+)$-(R)-1-methyl-4-(prop-2-en-1-yl)cyclohexene; $(-)$-limonene (lemon odor): $(-)$-(S)-1-methyl-4-(prop-2-en-1-yl)cyclohexene.

Figure 1 Examples of monoterpenes obtained from the pyrolysis of pine trees.

$(-)$-α-Pinene $(+)$-α-Pinene $(-)$-β-Pinene $(+)$-3-Carene

$(-)$-Camphene $(+)$-Limonene $(-)$-Limonene α-Terpinolene
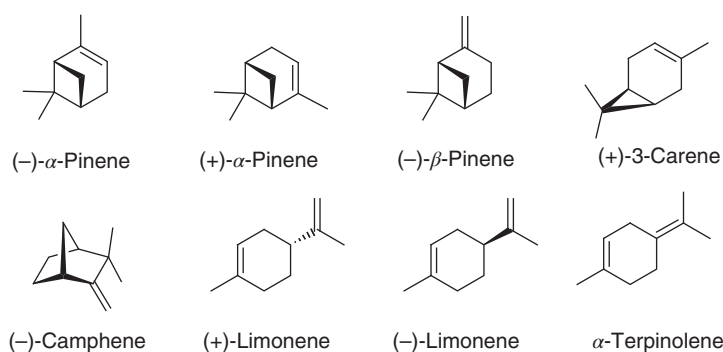
In 1800, about 500 organic compounds were known. Around 1850 pyrolysis (carbonization or destructive distillation) of hard coal produced many new substances, and this launched the chemical industry of organic compounds. When the first edition of Beilstein's Handbook of Organic Chemistry appeared in 1882, already 20 000 organic compounds were cited. Isolation of compounds from plants and animals also contributed to this number. In 1912, about 150 000 organic substances were known. Today, over 50 million chemicals have been registered. Pyrolysis of coal produces coke (70%), NH_3/H_2O(10%), coal gas (town gas: mostly H_2 and CH_4; contains lesser amounts of CO, ethane, ethylene, benzene, toluene, and cyclopentadiene) and coal tar as the main source of starting materials (benzene, toluene, phenols, anilines, pyridine, naphthalene, anthracene, phenanthrene, chrysene, carbazole, quinoline, and pyrrole) for the manufacture of soap, fats, dyes, plastics, perfumes, drugs, pesticides, explosives, etc. Industrial organic chemistry started with the manufacture of mauveine (a purple dying agent called also Perkin mauve, aniline purple, and Tyrian purple) suitable as a dye of silk and other textiles. In 1856, William Henry Perkin oxidized aniline using $K_2Cr_2O_7$ in H_2SO_4, whose toluidine impurities reacted with the aniline and yielded the dye (Figure 2) [1–4].

Invented in 1888, the industrial production of calcium carbide combines lime and coke in an electric arc furnace at 2000 °C. This highly endothermic reaction $(\Delta_r H^{298\,K}[CaO(solid) + C(graphite) \rightleftarrows CaC_2(solid) + CO(gas)] = 112\,kcal\,mol^{-1}$ [5] is possible because of the formation of CO that is eliminated while it forms (equilibrium shift). Calcium carbide reacts with water to give acetylene $(CaC_2 + H_2O \rightarrow CaCO_3 + H—C\equiv C—H)$, and with nitrogen to give calcium cyanamide $(CaC_2 + N_2 \rightarrow C + Ca^{++}/^-N=C=N^-)$, a fertilizer $(CaCN_2 + 3H_2O \rightarrow 2NH_3 + CaCO_3)$. Acetylene is an important compound used in welding (metal industry) and in the production of several chemicals such as acetaldehyde (MeCHO), acetic acid (MeCOOH), ethanol (MeCH_2OH), vinyl acetate $(H_2C=CH—OCOMe)$, vinyl chloride $(CH_2=CH—Cl)$, acrylic acid and esters $(CH_2=CHCOOR, R = H, alkyl)$, acrylonitrile $(CH_2=CH—C\equiv N)$, and chloroprene $(CH_2=CH—C(Cl)=CH_2)$. Except in China where the calcium carbide procedure enjoys a renaissance, acetylene is produced today utilizing natural gas or petroleum as sources.

Isoprene (2-methylbutadiene) was first obtained by the distillation of natural rubber [6, 7]. In 1835, Liebig observed that the most volatile fraction of rubber produces a high boiling (230 °C) oil by means of concentrated sulfuric acid [8]. In 1879, Bouchardat

Figure 2 The birth of the industry of organic chemistry is based on coal tar.

Mauveine A
(a phenazine derivative)

(a)

Isopent-2-en-1-yl pyrophosphate

Isopent-3-en-1-yl pyrophosphate
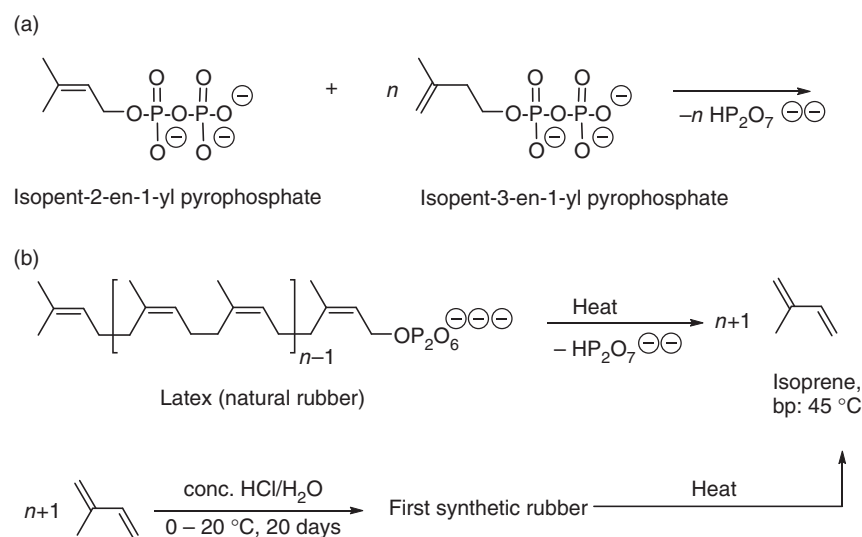
Figure 3 (a) Biosynthesis of natural rubber latex and its pyrolysis into isoprene and (b) protic-acid-induced polymerization of isoprene that produces synthetic rubber.

(b)

Latex (natural rubber)

Isoprene,
bp: 45 °C

First synthetic rubber

reported the polymerization of isoprene to an elastic product that again gave isoprene on distillation (Figure 3) [9]. This discovery opened the field of polymer chemistry that our civilization could not exist without today [10]. Thus, heat breaks C—C bonds in a large organic molecule (rubber is a long polymer with a molecular mass of 10^5–10^6) and produces smaller molecules; in this case, isoprene. In the presence of a suitable catalyst, the polymer can be formed again at a lower temperature. Isoprene is protonated by the protic acid equilibrating with 2-methylbut-3-en-2-yl cation intermediate that adds to another molecule of isoprene, giving an another carbocation intermediate that continues the polymerization process (an example of cationic polymerization).

Nowadays, petroleum is by far the most important raw material for producing chemicals. Although most of it is utilized for the manufacture of gasoline, diesel fuel, jet fuel, heating oil, and power plant fuel, 10% of it is used to produce chemicals. In refineries, petroleum is first rectified to give various fractions having different boiling temperatures. These fractions are then upgraded to fuels,

mostly applying catalytic processes. Steam cracking of hydrocarbons at c. 850 °C without catalyst produces mostly ethylene (CH_2=CH_2), propylene (Me—CH=CH_2), and by-products such hydrogen as (H_2), methane (CH_4), C_4 hydrocarbons (butane: Me—CH_2—CH_2—Me), isobutane: Me_2CHMe, (*E*)- and (*Z*)-but-2-ene: (*E*)-and (*Z*)-Me—CH=CH—Me, but-1-ene: Me—CH_2—CH=CH_2), and the "BTX-aromatics" (benzene: C_6H_6=Ph–H, toluene: PhMe, *ortho*-, *meta*-, and *para*-xylene: $C_6H_4Me_2$).

Reaction energy hypersurfaces

At the macroscopic level, any equilibrium at constant temperature T and pressure P is characterized by a Gibbs energy or free energy diagram (Figure 4) and an enthalpy diagram (Figure 5). Measurement of the equilibrium constant K^T gives $\Delta_r G^T$ and calorimetry provides $\Delta_r H^T$. Kinetics (measurement of the rate constant at different temperature, Section 3.2) gives the activation parameters $\Delta^{\ddagger} G^T$ and $\Delta^{\ddagger} H^T$ for the transition states with the highest free energy and enthalpy, respectively. For the

Figure 4 Free energy diagram (a) for an equilibrium that does not involve a reactive intermediate and (b) for an equilibrium that involves a single reactive intermediate. In this case, the rate-determining step (the slowest step) is associated with transition state $^{\ddagger}{}_1$, the highest in free energy.
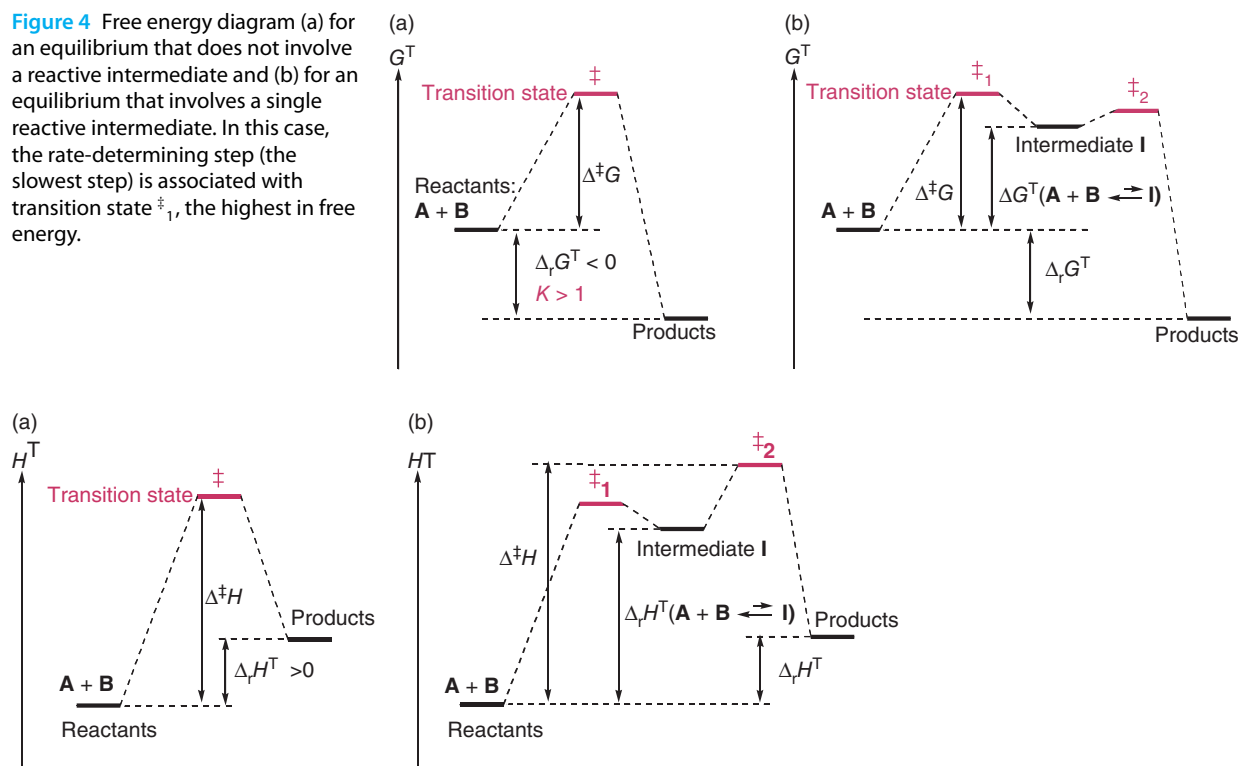
Figure 5 Enthalpy diagram for an equilibrium (a) that does not involve a reactive intermediate and (b) that involves a single reactive intermediate. In the case chosen, $^{\ddagger}{}_2$ is higher in enthalpy than $^{\ddagger}{}_1$, which corresponds to the transition state of the rate-determining step in the free energy diagram of Figure 4b. This is possible because of $\Delta^{\ddagger} G = \Delta^{\ddagger} H - T\Delta^{\ddagger} S$. Both reactions chosen here are endothermic ($\Delta_r H^T > 0$) and have a positive entropy variations ($\Delta_r S^T > 0$) making $\Delta_r G^T = \Delta_r H^T - T\Delta_r S^T < 0$. The reaction illustrated in Figures 4b and 5b has a more negative activation entropy ($\Delta^{\ddagger} S < 0$) for the slowest step involving transition state $^{\ddagger}{}_1$ than for $^{\ddagger}{}_2$.

other transition states and the intermediates that are involved in the reaction, their thermochemical data can be estimated by quantum mechanical calculations or by applying various theories on chemical activation. For neutral reactive intermediates such as radicals and diradicals, their standard heats of formation can be estimated readily from gas-phase homolytic bond dissociation enthalpies ($DH°(R^·/X^·)$). Therefore, $\Delta_r H°$(reactants $\rightleftarrows$ intermediate) can be obtained through a simple thermochemical calculation. To a first approximation entropy variations, $\Delta_r S°$(reactants $\rightleftarrows$ intermediate) is estimated readily by considering the change of number of species between the intermediate and the reactants, by considering their molecular masses and whether rotations about single bonds are lost or gained between the intermediate and the reactants. For reactions generating ion pairs such as acid/base equilibria, $\Delta_r G°$(reactants $\rightleftarrows$ intermediate) $= 1.36 \cdot (\Delta pK_a)$. For other heterolyses in solution, the gas-phase heterolytic bond dissociation enthalpies (e.g. ($DH°(R^+/X^-)$) can often be used applying well-defined corrections for reactions in solutions. In several instances, substituent effects on the relative stability of charged intermediates in the gas phase correlate with the substituent effects on the same species in solution. When a reaction has a relatively high barrier and a slowly varying entropy (e.g. an isomerization has a relatively small positive or negative $\Delta^‡ S$ value, a fragmentation has a slightly positive $\Delta^‡ S$ value; however, a reaction following an associative mechanism has a highly negative $\Delta^‡ S$ value) in the region of the transition state, its energy and geometry correspond closely to those of the reactive intermediate it is connected with. This is the Hammond postulate. In the case of Figure 5b, the reactive intermediate resembles in the geometry and enthalpy transition state $^‡_1$ that separates it from the reactants. It also resembles transition state $^‡_2$ that separates it from the products. This postulate is in fact a theorem demonstrated by the Bell–Evans–Polanyi theory and reflected in the Dimroth principle for one-step reactions: $\Delta^‡ H^T = \alpha \Delta_r H^T + \beta$ (with α varying between 0 and 1). The higher the exothermicity of a reaction, the lower its activation enthalpy. For a thermoneutral equilibrium ($\Delta_r H^T = 0$), $\Delta^‡ H^T = \beta$, the intrinsic barrier of the reaction that depends on steric factors, electronic factors (dipole/dipole interactions and electron exchange), and solvation.

At the molecular level, a chemical reaction may be represented in $N + 1$ dimensional space. One dimension represents the potential energy, E, of the system, whereas the other N dimensions are the coordinates that describe the geometries of the chemical species undergoing change. For a reaction involving a single,
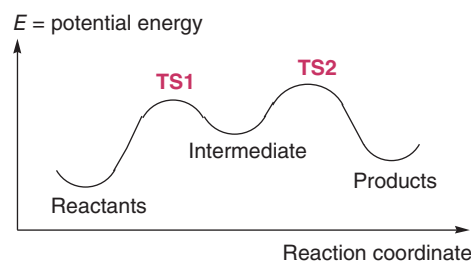
Figure 6 A one-dimensional slice through a reaction energy hypersurface (potential energy vs. reaction coordinate diagram) corresponds to the enthalpy diagram of Figure 5b.

nonlinear molecule, it takes $N = 3n - 6$ (coordinates where n = number of atoms in the molecule) to fully describe the molecule and the reaction. For example, each atom can be defined in space by an X, Y, and Z coordinate, giving $3n$ total coordinates. Only $3n - 6$ are needed to define the internal structure of a molecule, three more give the position of the molecule in space with respect to some reference, while three more tell how the molecule is oriented in space. The potential energy $E = f$(coordinates) will have minima, maxima, and saddle points as shown in Figure 6 for the two-step reaction illustrated in Figures 4b and 5b.

The minima correspond to reactants, products, or reactive intermediates (**I**), whereas the saddle points are transition structures TS1 and TS2 that are associated with the transition states $^‡_1$ and $^‡_2$ of the reaction, respectively.

Such a one-dimensional slice is just a glimpse of the whole story, as a full description of a molecule actually involves all $3n - 6$ internal coordinates. Energy *versus* reaction coordinate diagrams in Figure 6 show energy as a function of one coordinate change only. Quantum mechanical calculations incorporating the Born–Oppenheimer approximation (the motion of the nuclei can be separated from the motion of the electrons) can be applied to determine the potential energies E of molecules with any geometry of the nuclei. When a large number of these calculations are done, a potential energy hypersurface for vibrationless system is obtained. The most important regions of the multidimensional surface are those corresponding to stationary points, which have zero first derivatives of E with respect to the $3n - 6$ coordinates. Energy minima are a point for which all force constants (second derivatives of E with respect to the $3n - 6$ coordinates) are positive. The saddle points are the transition structures (Figure 7); they have one, and only one, negative second derivative, the remaining $3n - 7$ second derivatives are positive. The negative second derivation of E corresponds to a force constant
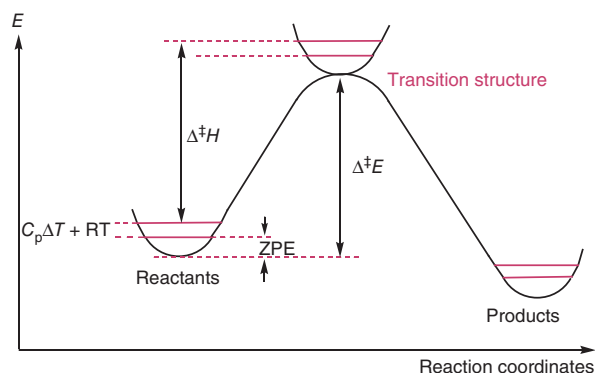
Figure 7 Relationship between $\Delta^{\ddagger}H$ (macroscopic activation parameter) and calculated $\Delta^{\ddagger}E$ (microscopic level) at $T > 0\,K$ along a reaction pathway. ZPE, zero-point energy and C_p, calorific capacity at constant pressure p.

for the motion along the reaction coordinate, which is referred to an "imaginary vibrational frequency" as the vibrational frequency is proportional to the square root of the force constant [11, 12].

When a reaction has a low barrier or rapidly varying entropy in the region of the potential energy maximum, the transition state may have a geometry different from that of the calculated transition structure. Furthermore, a transition state might be associated with more than one transition structure.

In 1931, about 40 years after Arrhenius's empirical observation, Eyring and Polanyi developed the first potential energy hypersurface for the degenerate reaction of hydrogen atom (H$^\cdot$) with dihydrogen (H$_2$) [13, 14]. Then, Hirschfelder, Eyring, and Topley performed the first trajectory calculation with femtosecond steps in 1936 [15]. These theoretical developments constituted the birth of reaction dynamics, and chemists began to think in terms of motions of atoms and molecules (dynamics) on potential energy surfaces. In 1973, Wang and Karplus [16] were the first to carry out a trajectory calculation of this type for a simple organic reaction: $CH_2 + H_2 \rightarrow CH_4$. Such calculations have become more commonplace, but only in the last decade have organic chemists begun to recognize how dynamics may alter the static picture of a reaction given by the potential surface [17].

The Arrhenius A frequency factor is typically 10^{13} Hz (per second) for a unimolecular reaction, a typical value of the frequency of a molecular vibration. In the mid-1930s, experimental temporal resolution of only seconds to milliseconds was possible in chemistry by means of the stopped-flow technique. Norrish and Porter [18] introduced in 1949 the flash photolysis technique reaching millisecond timescale.

By exposing a solution to a heat, pressure, or electrical shock (the so-called temperature-jump method, etc.), Eigen achieved microsecond (10^{-6} seconds) temporal resolution [19]. The advent of the pulsed nanosecond (10^{-9} seconds) laser in the mid-1960s [20, 21], and soon after of the picosecond (10^{-12} seconds) laser [22, 23], brought a million times improvement in temporal resolution of chemical elementary processes. However, even on the short picosecond timescale, molecular states already reside in eigenstates (the static limit), and only the change of population of that state with time is observable, not the change of geometry of the molecules. The advent of femtosecond (10^{-15} seconds) laser technology of Shank [24–26] finally opened the possibility to probe molecular motion and chemical reactions in real time [27]. Transition states as well as reactive intermediates can now be visualized as demonstrated by Zewail for a large number of chemical and biological processes [28–32]. Attosecond temporal resolution is now possible and even permits the observation of electron dynamics [33, 34].

Can we see reactions in real time?

To take what amounts to a movie of a simple chemical reaction, Zewail and coworkers used two beams of femtosecond pulses and a mass spectrometer. A first pulse of light, called the pump pulse, strikes the molecule and energizes it. If the photon energy is sufficient, it induces a chemical reaction that can break the molecule apart into molecular fragments. In order to follow the birth and order of appearance of these fragments, a second pulse traveling just a few femtoseconds behind the first hits the fragments and ionizes them. The nature of fragments can be followed by mass spectrometry. The second pulse, called the probe pulse, can be timed precisely at different intervals to reveal how long it takes for various chemical species to appear and in what order they do so. The experiment that gave birth to femtochemistry in 1987 involved the dissociation of cyanogen iodide (ICN), in which the appearance of a free CN fragment was found to occur in about 200 fs [35]. Figure 8 is a colorful popular presentation of the way Zewail's technique works, from the Nobel Prize lecture cover of the journal [36].

Laser irradiation of 1,2-diiodo-1,1,2,2-tetrafluoroethane generates a molecule of tetrafluoroethylene and two iodine radicals. The first C—I bond cleavage takes about 200 fs, whereas the second follows on a timescale 100 times longer [37]. This
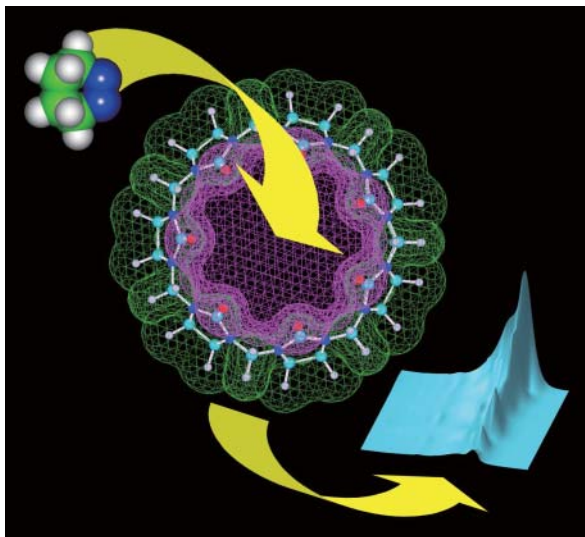
Figure 8 How Zewail's technique obtains a "movie" of a reaction. Source: Drawing supplied by Werner M. Nau, International University, Bremen, Germany.

Figure 9 Two possible mechanisms for the thermal $(2 + 2)$ cycloreversion of cyclobutane to ethylene. (a) a stepwise intermediate involving a diradical intermediate and two transition states; (b) a concerted mechanism involving one transition state.

demonstrates that the photoinduced fragmentation is a two-step process with the formation of a 1,1,2,2-tetrafluoro-2-iodoethyl radical intermediate. This conclusion may, or may not, apply to a reaction in solution induced by heating but provides a fast snapshot of the radical process in the gas phase [38].

Concerted or nonconcerted?

For the past 70 years, the concept of diradicals as intermediates of reactions has been considered as the archetype of chemical transformations in many classes of thermally activated, as well as photochemical, reactions, including the broad class of pericyclic reactions (Chapter 5). In one classical example, the ring opening of cyclobutane and its fragmentation into two molecules of ethylene ((2+2)-cycloreversion) may proceed directly through a transition state at the saddle point of an activation barrier (Figure 9a) or through a two-step, nonconcerted mechanism involving first the cleavage of one of the $\sigma(C—C)$ bonds to yield a tetramethylene diradical (buta-1,4-diyl diradical) intermediate (Figure 9b). A reactive intermediate is expected to be longer lived than a transition state, such that the dynamics of its nuclear motion (vibration and rotation), unlike a concerted motion (translation), determines the outcome of the reaction.

By combining femtosecond spectroscopy with time-of-flight mass spectrometry and molecular beams, and by generating the diradical from an alternate source, Zewail and coworkers established the existence of this 1,4-diradical (Figure 9a) as a distinct molecular species [39]. Femtochemistry has been applied to the condensed phase to pinpoint the details of solvation dynamics and to biomolecules [40, 41]. It provides insight into the function of biological systems. The ability to visualize motion in a protein enables one to study the relationship between nuclear motion and biological functions. As an example, it is known that hydrogen bonds bind the double-stranded DNA helix and determine the complementarity of pairing. With ultrafast laser spectroscopy, Zewail and coworkers have identified different timescales of the structural relaxation and cooling of the tautomers [42–44]. These studies have demonstrated that we can now watch reactions occur in ideal systems, and they give us the hope that one day we will obtain a detailed molecular picture of the nuclear dynamics that govern the fundamentals of chemical reactivity in biological systems. Femtochemistry has been applied to the study of reactions at metal surfaces [45–47].

Structures of species on the reaction hypersurface

In an ultrafast laser experiment, the data collected do not give the direct structure of the species under study, as fluorescence or mass spectra have to be translated into structures. Actually, the only species well characterized on a reaction hypersurface are the

starting materials (or reactants) and the final products that are long-lived and thus can be analyzed by X-ray crystallography and neutron diffraction for crystalline compounds or by electron diffraction for gaseous substances. In some cases, reactive intermediates can be "frozen out" by some special techniques and thus analyzed as any other substances. The geometry of a transition state cannot be analyzed by these means as it is too short-lived (less than the time necessary to a molecular vibration, by definition; 300 fs for the conversion of (*Z*)-stilbene into its (*E*)-isomer). Transition structures must be inferred from theories and models, and by the interpretation of spectroscopic fingerprints in the case of ultrafast laser spectroscopy.

At 25 °C, simple molecules or atoms of a gas travel with a speed of 10^4–10^5 cm s^{-1} (i.e. 10^{12}–10^{13} Å s^{-1}). The lifetime of an activated complex (or transition state) [48] resulting from the collision of molecule **AB** with **C** to generate products, **A** + **BC**, can be estimated as follows. The distance traveled by the ensemble **AB** + **C** undergoing through the activated complex [48] to give product **A** + **BC** amounts

to about 1–10 Å or 0.1–1 nm (10^{-9} m), which, at 10^{12}–10^{13} Å s^{-1}, requires about 10^{-13}–10^{-11} seconds (100 fs to 10 ps) [49]. The timescale for movements of valence electrons is 10^{-17} seconds (10 as), and for molecular rearrangements by movements of nuclei, 10^{-13} seconds (100 fs) [34, 50].

Through a combination of light and electron probes, it is possible to record single-molecule dynamics with simultaneous sub-angstrom spatial and femtosecond temporal resolution. Single-molecule femtochemistry is becoming possible through a melding of laser spectroscopy and electron microscopy techniques [51, 52]. The computational study of organic reaction dynamics is becoming increasingly common, and a time-resolved understanding of the timing of bond formation has enriched our views of the details of organic reaction mechanisms [53, 54].

Lausanne, June 1st, 2019   *Pierre Vogel*
Los Angeles, June 1st, 2019   *Kendall N. Houk*

References

1 Perkin, W.H. On mauvein and allied colouring matters. *Journal of the Chemical Society, Transactions* 1879: 717–732.

2 Travis, A.S. (1990). Perkins Mauve – ancestor of the organic-chemical industry. *Technology and Culture* 31 (1): 51–82.

3 Huebner, K. (2006). History – 150 years of mauveine. *Chemie in unserer Zeit* 40 (4): 274–275.

4 Sousa, M.M., Melo, M.J., Parola, A. et al. (2008). A study in mauve: unveiling Perkin's dye in historic samples. *Chemistry - A European Journal* 14 (28): 8507–8513.

5 Geiseler, G. and Buchner, W. (1966). Uber Die Bildungsenthalpie des Calciumcarbids. *Zeitschrift für Anorganische und Allgemeine Chemie* 343 (5–6): 286–293.

6 Whitby, G.S. and Katz, M. (1933). Synthetic rubber. *Industrial and Engineering Chemistry* 25: 1204–1211.

7 Whitby, G.S. and Katz, M. (1933). Synthetic rubber (concluded). *Industrial and Engineering Chemistry* 25: 1338–1348.

8 von Liebig, J. (1835). Bemerkung über die methoden der Darstellung und Reinigung flüchtiger, durch trockene destillation organischer materien erhaltene producte. *Annalen der Pharmacie* 16 (1): 61–62.

9 Bouchardat, G. (1879). Action des hydracides sur l'isoprène; reproduction du caoutchouc. *Comptes rendus hebdomadaires des séances de l'Académie des Sciences Paris* 89: 1117–1120.

10 Long, J.C. (2001). The history of rubber – a survey of sources about the history of rubber. *Rubber Chemistry and Technology* 74 (3): 493–508.

11 Hehre, W.J., Radom, L., Schleyer, P.v.R., and Pople, J.A. (1986). *Ab initio Molecular Orbital Theory*. New York: Wiley.

12 Simons, J. (1991). An experimental chemists guide to *ab initio* quantum-chemistry. *Journal of Physical Chemistry* 95 (3): 1017–1029.

13 Eyring, H. and Polanyi, M. (1931). Concerning simple gas reactions. *Zeitschrift fuer Physikalische Chemie* B12 (4): 279–311.

14 Polanyi, M. (1932). *Atomic Reactions*. London: Williams and Norgate.

15 Hirschfelder, J., Eyring, H., and Topley, B. (1936). Reactions involving hydrogen molecules and atoms. *Journal of Chemical Physics* 4 (3): 170–177.

16 Wang, I.S.Y. and Karplus, M. (1973). Dynamics of organic reactions. *Journal of the American Chemical Society* 95 (24): 8160–8164.

17 Carpenter, B.K. (1998). Dynamic behavior of organic reactive intermediates. *Angewandte Chemie International Edition* 37 (24): 3340–3350.

18 Norrish, R.G.W. and Porter, G. (1949). Chemical reactions produced by very high light intensities. *Nature* 164 (4172): 658–658.

19 Eigen, M. (1954). Methods for investigation of ionic reactions in aqueous solutions with half-times as short as 10^{-9} s – application to neutralization and hydrolysis reactions. *Discussions of the Faraday Society* 17: 194–205.

20 Hellwarth, R.W. (1961). *Advances in Quantum Electronics*. New York: Columbia University Press.

21 McClung, F.J. and Hellwarth, R.W. (1962). Giant optical pulsations from ruby. *Journal of Applied Physics* 33 (3): 828–829.

22 Hargrove, L.E., Fork, R.L., and Pollack, M.A. (1964). Locking of He–Ne laser modes induced by synchronous intracavity modulation (diffraction by phonons in crystals e). *Applied Physics Letters* 5 (1): 4–5.

23 McDuff, O.P. and Harris, S.E. (1967). Nonlinear theory of internally loss-modulated laser. *IEEE Journal of Quantum Electronics* QE 3 (3): 101–111.

24 Shank, C.V. (1988). *Ultrashort Laser Pulses*. Berlin: Springer-Verlag.

25 Shank, C.V. (1986). Investigation of ultrafast phenomena in the femtosecond time domain. *Science* 233 (4770): 1276–1280.

26 Zewail, A.H. (2000). Femtochemistry: atomic-scale dynamics of the chemical bond. *Journal of Physical Chemistry A* 104 (24): 5660–5694.

27 Leone, S.R., McCurdy, C., Burgdoerfer, J. et al. (2014). What will it take to observe processes in 'real time'? *Nature Photonics* 8 (3): 162–166.

28 Zewail, A.H. and Bernstein, R.B. (1988). Special report – real-time laser femtochemistry – viewing the transition from reagents to products. *Chemical & Engineering News* 66 (45): 24–43.

29 Khundkar, L.R. and Zewail, A.H. (1990). Ultrafast molecular reaction dynamics in real-time – progress over a decade. *Annual Review of Physical Chemistry* 41: 15–60.

30 Zewail, A.H. (1993). Femtochemistry. *Journal of Physical Chemistry* 97 (48): 12427–12446.

31 Zewail, A.H. (1990). The birth of molecules. *Scientific American* 263 (6): 76–82.

32 Zewail, A.H. (2000). Femtochemistry. Past, present, and future. *Pure and Applied Chemistry* 72 (12): 2219–2231.

33 Kling, M.F. and Vrakking, M.J. (2008). Attosecond electron dynamics. *Annual Review of Physical Chemistry* 59: 463–492.

34 Sansone, G., Kelkensberg, F., Perez-Torres, J. et al. (2010). Electron localization following attosecond molecular photoionization. *Nature* 465 (7299): 763–766.

35 Dantus, M., Rosker, M.J., and Zewail, A.H. (1988). Femtosecond real-time probing of reactions. 2. The dissociation reaction of ICN. *Journal of Chemical Physics* 89 (10): 6128–6140.

36 Zewail, A.H. (2000). Femtochemistry: atomic-scale dynamics of the chemical bond using ultrafast lasers – (Nobel lecture). *Angewandte Chemie International Edition* 39 (15): 2586–2631.

37 Khundkar, L.R. and Zewail, A.H. (1990). Picosecond photofragment spectroscopy. 4. Dynamics of consecutive bond breakage in the reaction $C_2F_4I_2 \rightarrow C_2F_4 + 2I$. *Journal of Chemical Physics* 92 (1): 231–242.

38 Carley, R.E., Heesel, E., and Fielding, H.H. (2005). Femtosecond lasers in gas phase chemistry. *Chemical Society Reviews* 34 (11): 949–969.

39 Pedersen, S., Herek, J.L., and Zewail, A.H. (1994). The validity of the diradical hypothesis – direct femtosecond studies of the transition-state structures. *Science* 266 (5189): 1359–1364.

40 Brixner, T. and Gerber, G. (2003). Quantum control of gas-phase and liquid-phase femtochemistry. *ChemPhysChem* 4 (5): 418–438.

41 Brixner, T., Damrauer, N.H., Kiefer, B., and Gerber, G. (2003). Liquid-phase adaptive femtosecond quantum control: removing intrinsic intensity dependencies. *Journal of Chemical Physics* 118 (8): 3692–3701.

42 Douhal, A., Kim, S.K., and Zewail, A.H. (1995). Femtosecond molecular-dynamics of tautomerization in model base-pairs. *Nature* 378 (6554): 260–263.

43 Fiebig, T., Chachisvilis, M., Manger, M. et al. (1999). Femtosecond dynamics of double proton transfer in a model DNA base pair: 7-azaindole dimers in the condensed phase. *Journal of Physical Chemistry A* 103 (37): 7419–7431.

44 Wan, C.Z., Fiebig, T., Schiemann, O. et al. (2000). Femtosecond direct observation of charge transfer between bases in DNA. *Proceedings of the National Academy of Sciences of the United States of America* 97 (26): 14052–14055.

45 Frischkorn, C. and Wolf, M. (2006). Femtochemistry at metal surfaces: nonadiabatic reaction dynamics. *Chemical Reviews* 106 (10): 4207–4233.

46 Mehlhorn, M., Gawronski, H., Nedelmann, L. et al. (2007). An instrument to investigate femtochemistry on metal surfaces in real space. *Review of Scientific Instruments* 78 (3): 033905.

47 Petek, H. (2012). Photoexcitation of adsorbates on metal surfaces: one-step or three-step. *Journal of Chemical Physics* 137 (9): 091704.

48 Tommos, C. and Babcock, G.T. (2000). Proton and hydrogen currents in photosynthetic water oxidation. *Biochimica et Biophysica Acta-Bioenergetics* 1458 (1): 199–219.

49 Polanyi, J.C. and Zewail, A.H. (1995). Direct observation of the transition-state. *Accounts of Chemical Research* 28 (3): 119–132.

50 Bucksbaum, P.H. (2007). The future of attosecond spectroscopy. *Science* 317 (5839): 766–769.

51 Lee, J., Perdue, S.M., Perez, A.R., and Apkarian, V.A. (2014). Vibronic motion with joint angstrom-femtosecond resolution observed through fano progressions recorded within one molecule. *ACS Nano* 8 (1): 54–63.

52 Petek, H. (2014). Single-molecule femtochemistry: molecular imaging at the space-time limit. *ACS Nano* 8 (1): 5–13.

53 Yang, Z. and Houk, K.N. (2018). The Dynamics of Chemical Reactions: Atomistic Visualizations of Organic Reactions, and Homage to van't Hoff. *Chem. Eur. J.* 24: 3916–3924.

54 Yang, Z., Jamieson, C.S., Xue, X.-S., Garcia-Borras, M., Benton, T., Dong, X., Liu, F. and Houk, K.N. (2019). Mechanisms and Dynamics of Reactions Involving Entropic Intermediates *Trends in Chemistry*. 1: 22–34.